A Sensitivity Study of a Torque Modulation-Based Friction Coefficient Estimation Between the Wheel-Rail Contact

Manakshya, Nikhil; Yu, Xinxin; Wang, Hongrui; Núñez, Alfredo; Dollevoet, Rolf; Zoeteman, Arjen; Li, Zili

Publication date
2025

Document Version
Final published version

Citation (APA)
Manakshya, N., Yu, X., Wang, H., Núñez, A., Dollevoet, R., Zoeteman, A., & Li, Z. (2025). *A Sensitivity Study of a Torque Modulation-Based Friction Coefficient Estimation Between the Wheel-Rail Contact*. Paper presented at World Congress of Railway Research 2025, Colorado Springs, Colorado, United States.

WCRR 2025
THE BROADMOOR, COLORADO SPRINGS, CO, USA
NOVEMBER 17-21, 2025

A Sensitivity Study of a Torque Modulation-Based Friction Coefficient Estimation Between the Wheel-Rail Contact

Nikhil Manakshya[1], Xinxin Yu[1], Hongrui Wang[1], , Alfredo Núñez[1] ,Rolf Dollevoet[1], Arjen Zoeteman[1,2], Zili Li[1]

[1] Section of Railway Engineering, Delft University of Technology, 2628CN Delft, The Netherlands
[2]ProRail, 3511EP Utrecht, The Netherlands

Abstract

The coefficient of friction (COF), defined as the maximum of the adhesion coefficient for a given contact condition, fluctuates rapidly due to environmental and operational factors. This paper introduces a torque modulation-based method for COF estimation. A simplified analytical model of the Manchester benchmark bogie operating under dry adhesion conditions is used to evaluate this method. The study presents an analytical equation that confirms earlier simulation-based findings showing a phase difference between applied torque modulation and resulting motor angular velocity. This phase relationship is shown to reflect the shape of the adhesion-slip curve. Notably, when the phase difference approaches 90°, the locomotive operates near the point of maximum adhesion, corresponding to the COF. Furthermore, the sensitivity of this approach to key system parameters, including normal load, wheel rolling radius, and modulation frequency, is examined. The findings provide valuable insights into the robustness and applicability of torque modulation-based COF estimation techniques in real-time traction control systems. The estimated COF can be further leveraged for adhesion management, driver advisory systems, and autonomous train operation.
Keywords: COF estimation, Torque modulation, Sensitivity analysis

1. Introduction

The coefficient of friction (COF), defined as the maximum of the adhesion coefficient *(μ)* for a given wheel–rail contact condition, is critical for traction and braking. Accurate COF estimation is challenging due to its sensitivity to rapidly changing factors such as rail surface conditions, slip velocity, and normal contact force. These challenges underscore the need for robust and reliable COF estimation methods, which is the focus of this paper. Low COF, often due to seasonal effects such as leaf contamination in autumn, can extend braking distances and necessitate speed restrictions, causing delays and reduced network efficiency. Without real-time COF estimation, operators must rely on conservative assumptions to adjust timetables and service frequency.

The adhesion force, which dictates traction and braking effort, is the product of the real-time adhesion coefficient and the normal force. It varies across the train's operational phases: maximum acceleration (MA), cruising (CR), and maximum braking (MB), as shown in Figure 1(a). This figure assumes maximum adhesion for dry rail (COF = 0.28) during MA and MB, without inducing wheel slip [1]. In these phases, real-time COF estimation is critical for ensuring optimal performance and safety.

A practical challenge in estimating COF lies in the estimation of slip velocity (v_s), which is defined as

$$v_s = r_w\omega - v_L \tag{1}$$

where r_w is the wheel radius, ω is the angular speed of the wheel, and v_L is the longitudinal velocity of the vehicle. Because v_s is often small and varies with dynamic wheel–rail interactions, precise measurement is difficult [2]. In practice, the difficulty lies in obtaining a reliable estimate of v_L, as sensors such as Doppler radar, inertial measurement units (IMUs), and GPS are susceptible to delays, noise, and environmental disturbances. The adhesion-slip relationship is commonly modelled using empirical expressions such as

$$\mu(v_s) = sign(v_s)(ce^{(-av_s)} - de^{(-bv_s)}) \tag{2}$$

where *a, b, c, and d* are experimentally determined coefficients representing different surface conditions. $sign(v_s)$ is a sign function applied to the slip velocity, such that the adhesion coefficient is negative during braking, whereas it is positive for traction. This formula is widely referenced in the literature [3] [4] [5]. Table 1 lists several coefficient sets and their corresponding rail surface condition applicable to Equation (2).

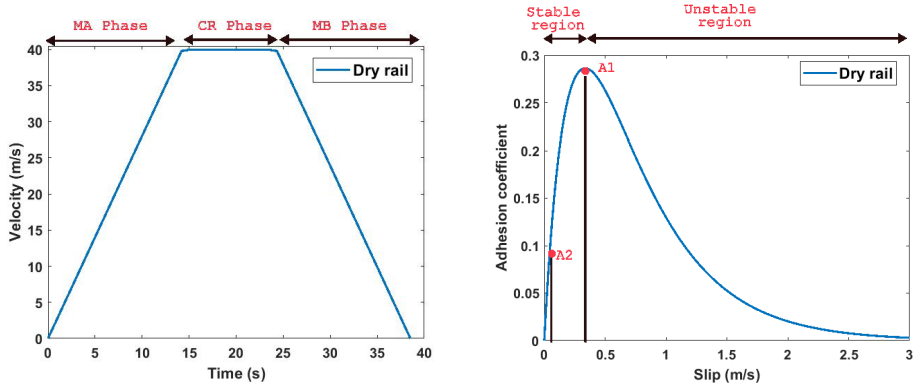

(a) Velocity profile of the vehicle based on dry curve (b) Adhesion slip curve for dry rail

Figure 1: Vehicle velocity and adhesion characteristics on dry rail

Rail Surface Condition	*a*	*b*	*c*	*d*
Dry Rail	0.54	1.2	1.0	1.0
Wet Rail	0.54	1.2	0.1	0.1
Wet Dew	0.05	0.5	0.08	0.08

Table 1: Rail surface conditions coefficients

Figure 1 (b) illustrates an adhesion slip relation using the dry rail surface condition from Table 1, highlighting two key points: A1 and A2. Point A1 corresponds to a COF of 0.28 and represents the desired operating point during the MA and MB phases, whereas point A2 reflects a lower adhesion requirement, typically used during the CR phase. The adhesion-slip curve in Figure 1 (b) also shows a clear distinction between stable and unstable regions. The stable region of the adhesion–slip curve is where the adhesion force increases with the slip. In contrast, the unstable region begins after the peak, where additional slip causes a rapid and uncontrolled decrease in adhesion force. Operating within the stable region is essential to avoid excessive slip, which otherwise leads to heat, noise, vibration, and wear of both wheel and rail.

2. COF Estimation Methods

Pichlik et al. [6] categorizes several slip control strategies capable of estimating COF. These methods aim to identify the optimal slip point, the point where the slope of the adhesion-slip curve approaches zero, corresponding to the COF. Three major approaches are briefly discussed below:

2.1. Slope-Based Estimation

Slope-based estimation is one of the most commonly used methods for identifying the COF, where the derivative $d\mu/dv_s$ is monitored to detect the peak of the adhesion–slip curve. Ohishi et al. [7] proposed a first-order observer that maintains operation near the point of maximum adhesion, where $d\mu/dv_s = 0$. Uyulan et al. [8] further developed this approach by incorporating a sliding-mode observer to regulate slip velocity based on the estimated slope.

While these methods are conceptually effective, they face two significant challenges. First, their accuracy depends on reliable estimation of slip velocity and adhesion, which relies on multiple measured signals such as motor torque, wheel speed, and longitudinal velocity, as well as system parameters like effective rolling radius, effective inertia and, resistance that are often assumed constant but vary with operating conditions and wear.

Second, estimating the slope requires computing derivatives such as $d\mu/dt$ and dv_s/dt, which introduces high-frequency noise and amplifies sensor errors, especially in the presence of signal disturbances or measurement delays.

2.2. Vibration-Based Estimation

Mei et al. [9] proposed using torsional vibration in the drive system, where pole shifts in the system matrix indicate the transition into unstable adhesion zones. While effective, this method relies on detecting vibration signatures using wheel-mounted speed sensors, which adds hardware complexity. Moreover, it requires a predefined threshold for vibration amplitude, which may not generalize well across different vehicle configurations or operating conditions.

2.3. Phase-Shift Estimation

Another noteworthy approach involves measuring the phase difference between motor torque modulation and wheel speed. As slip increases, this phase difference grows, reaching approximately 90° at the COF point. Central to this paper, the method enables real-time COF estimation using only internal motor drive signals, torque and speed, eliminating the need for slip observers or additional sensors. This concept has also been investigated in earlier studies [10], [11]. While building on similar principles, this study is supported by a simplified simulation framework (Figure 2), which provides clearer physical insight into the interaction between key variables. The resulting phase shift curve (Figure 3(b)) shows qualitative differences, more closely aligning with [10] than with [11], potentially due to the use of a more realistic adhesion–slip model in this study. Additionally, this paper uniquely includes a sensitivity analysis that quantifies the impact of system parameters such as normal load, wheel radius, and modulation frequency, an aspect not covered in the previous works.

3. Extended wheelset multi-axle model

Building upon a single-axle model, a multi-axle simulation model was developed using the parameters from a Manchester benchmark [12]. As shown in Figure 2, the current model includes two powered wheelsets connected via a bogie. Each wheelset receives torque input and interacts with the rail via its wheel-rail contact dynamics, allowing the simulation of different adhesion conditions for each wheelset.

The fundamental equations that guide the model are

$$\begin{aligned} F_m - F_a &= \frac{dv_w}{dt} M_w \\ 2F_a &= \frac{dv_L}{dt} M_{eq} \\ F_m &= T_m / r_w \\ F_a &= \mu(v_s) N \end{aligned} \tag{3}$$

where F_m is the motor force applied at the wheels, F_a is the adhesion force, v_w which is equal to $r_w\omega$ is the longitudinal speed of the wheels at the contact location, M_w is the equivalent mass reflected at each wheelset, M_{eq} is the total mass carried forward by the bogie, N which is equal to $M_{eq}/2 \times g$ is the normal load acting on each wheelset, T_m is the applied torque at the wheelset and, $\mu(v_s)$ is the adhesion coefficient that varies with the slip velocity. The wheel velocity v_w is then subtracted from the vehicle velocity v_L that provides the slip velocity v_s. The value of the parameters used in the model is mentioned in Table 2.

Parameter	Value	Unit
Meq	22241	Kg
r_w	0.46	m
M_w	1867	Kg

Table 2: Value of parameters used in the Simulink model

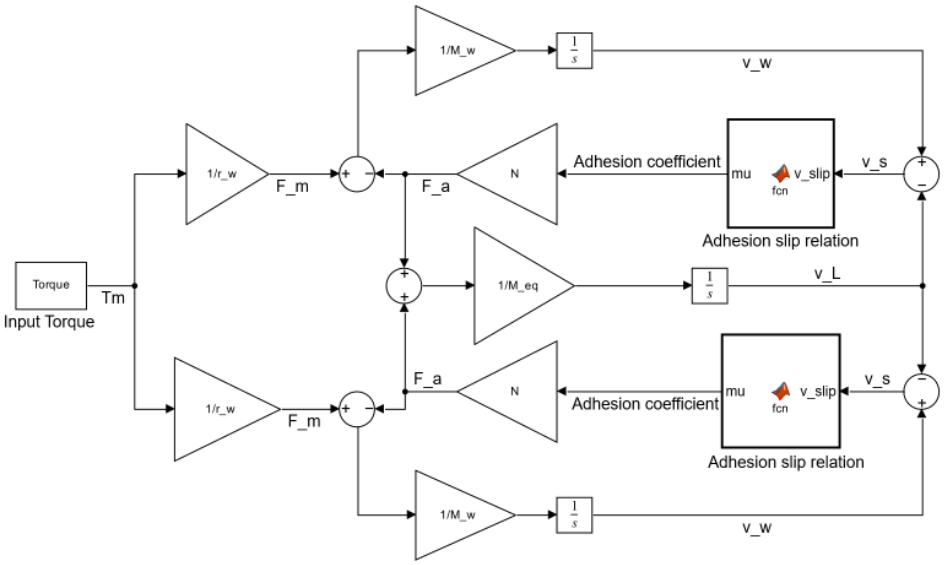

Figure 2: Two-wheelset model of the Manchester benchmark in Simulink

4. Torque modulation-based COF approach

The Torque modulation approach involves sinusoidal modulation of the input torque at a specific modulation frequency ω_m.

$$T_m(t) = T_o + \Delta T_o \, sin(\omega_m t) \tag{4}$$

where T_o is the mean torque and ΔT_o is the modulation amplitude. After linearizing (3) around an equilibrium operating point ω_o, the transfer function (TF) between ΔT and $\Delta\omega$ for a small-signal frequency analysis is:

$$\Delta\omega(s) = \frac{\Delta T(s)}{J_w(s+\alpha)} + \frac{\beta \Delta v_L}{J_w(s+\alpha)} \tag{5}$$

Where J_w is the reflected inertia at the wheelset and α and β is as shown below:

$$\alpha = (\frac{d\mu}{dv_s})\frac{{r_w}^2 N}{J_w}$$

$$\beta = (\frac{d\mu}{dv_s})N r_w$$

If the longitudinal velocity is constant, the second term in (5) becomes zero, and the TF simplifies to:

$$G(s) = \frac{1}{J_w(s+\alpha)}$$

For s=$j\omega_m$, the argument of the transfer function, which is also the phase difference between the applied torque and wheel velocity, is:

$$\phi(\omega_m) = \pm arctan(\frac{\omega_m}{\alpha}) \tag{6}$$

The phase difference is positive during traction and negative during braking. Equation (6) was shown in [11] for the case of constant velocity, which supports the validity of the present derivation.

5. Results and Discussions

The model in Figure 2 was evaluated at a constant velocity of 10 m/s. Initially, equal torque was applied to both wheelsets to accelerate the vehicle. Subsequently, 24 discrete step torques were applied, with one wheelset receiving a positive torque and the other an equal negative torque, thereby maintaining a constant vehicle velocity as shown in Figure 3 (a). Each step torque lasted for two seconds, consisting of one second of constant torque followed by one second of torque modulation. During the modulation phase, the average phase angle, slip, and adhesion coefficient were recorded based on the final two waveforms. The resulting variation of the phase angle is presented in Figure 3 (b).

Figure 3(b) highlights two key findings. First, it shows that the phase difference between torque and wheel

velocity increases with slip, ranging from approximately 13° to 90° along the dry adhesion curve, indicating the locomotive operating point and eliminating the need to estimate the slope of the adhesion-slip curve. Second, the close agreement between simulation and analytical results validates the proposed approach. In this analysis, all parameters were held constant except for the adhesion-slip slope, which varied with slip velocity.

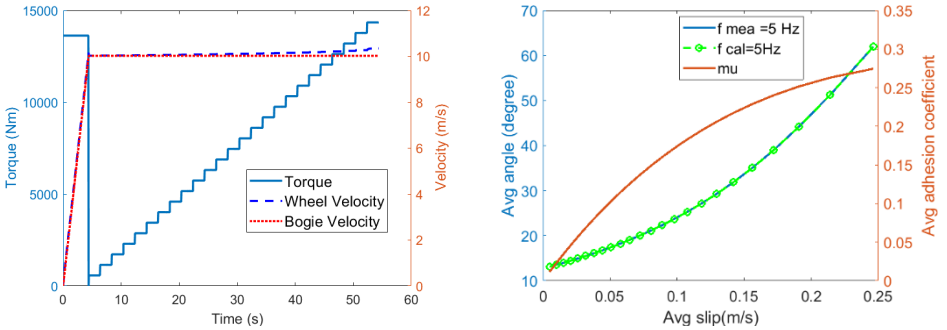

(a) Step torque after 10 m/s (b) Comparison between calculated and simulated angle

Figure 3: Result of the phase angle calculation by applying 24-discrete-step torque

The effect of equivalent mass, rolling radius, and modulation frequency from (6) on the phase angle is shown in Figure 4. It is essential to assess typical ranges of parameters like normal load and wheel radius to identify whether phase angle variations stem mainly from adhesion-slip slope or other parameters.

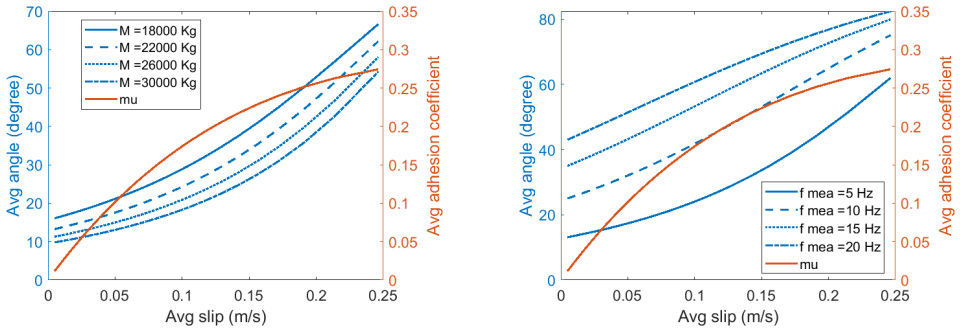

(a) Variation in M_{eq} at 5 Hz and r_w=0.46 m (b) Variation in freq with M_{eq} =22241 Kg and r_w=0.46 m

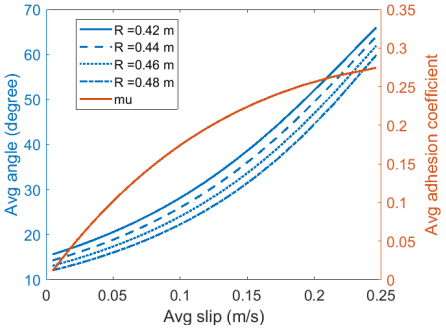

(c) Variation in r_w at 5 Hz and M_{eq} =22241 Kg

Figure 4: Variation of phase angle with vehicle mass, frequency, and wheel radius

6. Conclusion

This paper presents a torque modulation-based approach for real-time estimation of the COF in a multi-axle locomotive model. Using a model of the Manchester benchmark, the method estimates COF by analyzing the phase difference between applied torque and resulting wheel angular velocity, eliminating the need for slope estimation or slip observers. However, the method introduces several practical considerations, including low-frequency excitation from the modulation, which requires careful frequency selection, and added drivetrain stress, necessitating selective use. A load observer is still necessary, and control blocks, such as a phase angle

controller, may increase system complexity. Despite these challenges, the method is promising as it relies only on measurable drive signals, making it suitable for real-time traction control.

Acknowledgment

This research was partly supported by ProRail and Europe's Rail Flagship Project IAM4RAIL - Holistic and Integrated Asset Management for Europe's RAIL System under Grant Agreement No 101101966. Funded by the European Union. Views and opinion expressed are however those of the author(s) only and do not necessarily reflect those of the European Union or Europe's Rail Joint Undertaking. Neither the European Union nor the granting authority can be held responsible for them. The project FP3-IAM4Rail is supported by the Europe's Rail Joint Undertaking and its members.

References

[1] G.M. Scheepmaker, H.Y. Willeboordse, J.H. Hoogenraad, R.S. Luijt, and R.M.P. Goverde, "Comparing train driving strategies on multiple key performance indicators," *Journal of Rail Transport Planning & Management*, vol. 13, pp. 100–149, 2020.

[2] J. Zdenek and P. Pichlik, "Adhesion force detection method based on the Kalman filter for slip control purpose," *Journal of Control, Measurement, Electronics, Computing and Communications*, vol. 60, pp. 148–153, 2016.

[3] S. Wang, J. Xiao, J. Huang, and H. Sheng, "Locomotive wheel slip detection based on multi-rate KF," *Journal of the Franklin Institute*, vol. 353, pp. 4354–4370, 2016.

[4] Y. Takaoka and A. Kawamura, "Disturbance observer-based adhesion control for Shinkansen," in *Proceedings of the IEEJ Annual Conference*, Nagoya, Japan, 2000.

[5] A. Kawamura, T. Furuya, and K. Takeuchi, "Maximum adhesion control for Shinkansen using the tractive force tester," in *Proceedings of the IEEJ Industry Applications Society Conference*, Osaka, Japan, 2002.

[6] J. Zdenek and P. Pichlik, "Comparison of locomotive adhesion force estimation methods for a wheel slip control purpose," in *Proceedings of the 9th International Conference on Electronics, Computers and Artificial Intelligence (ECAI)*, Targoviste, Romania, 2017, pp. 1–6.

[7] K. Ohishi, Y. Ogawa, I. Miyashita, and S. Yasukawa, "Anti-slip re-adhesion control of electric motor coach based on force control using disturbance observer," in *Conference Record of the 2000 IEEE Industry Applications Conference*, vol. 4, pp. 2263–2268, 2000.

[8] M. Gokasan and C. Uyulan, "Modeling, simulation and re-adhesion control of an induction motor based railway electric traction system," *Proceedings of the Institution of Mechanical Engineers, Part I: Journal of Systems and Control Engineering*, vol. 232, pp. 3–15, 2018.

[9] N. Bosso, M. Spiryagin, A. Gugliotta, and A. Soma, "A mechatronic approach for anti-slip control in railway," in *IFAC Proceedings Volumes*, vol. 41, pp. 3541–3546, 2008.

[10] J. Bauer, "Controlled induction motor drive in railway traction," Master's thesis, Czech Technical University in Prague, 2020.

[11] G.J. Krishnan, Z. Yang, Z. Li, and R. Dollevoet, "Torque modulation-based train-borne measurement of coefficient of friction," in *Proc. Advances in Dynamics of Vehicles on Roads and Tracks III*, Cham, Switzerland: Springer, 2025, pp. 546–554.

[12] S. Iwnick, "Manchester benchmarks for rail vehicle simulation," *Vehicle System Dynamics*, vol. 30, pp. 295–313, 1998.